In situ diffusion test of hydrogen gas in the Opalinus Clay

A. VINSOT[1]*, C. A. J. APPELO[2], M. LUNDY[1], S. WECHNER[3], Y. LETTRY[4], C. LEROUGE[5], A. M. FERNANDEZ[6], M. LABAT[7], C. TOURNASSAT[5], P. DE CANNIERE[8], B. SCHWYN[9], J. MCKELVIE[10], S. DEWONCK[1], P. BOSSART[11] & J. DELAY[1]

[1]*Andra, CMHM, F-55290 Bure, France*

[2]*NL-1071 MB Amsterdam, The Netherlands*

[3]*Hydroisotop GmbH, D-85301 Schweitenkirchen, Germany*

[4]*Solexperts AG, CH-8617 Mönchaltorf, Switzerland*

[5]*BRGM, F-45060 Orléans, France*

[6]*Ciemat, S-28040 Madrid, Spain*

[7]*IRD, AMU-MIO, F-13288 Marseille, France*

[8]*FANC, B-1000 Brussels, Belgium*

[9]*Nagra, CH-5430 Wettingen, Switzerland*

[10]*NWMO, Toronto, ON, M4T 2S3, Canada*

[11]*Swisstopo, CH-2882 St-Ursanne, Switzerland*

**Corresponding author (e-mail: agnes.vinsot@andra.fr)*

Abstract: Hydrogen gas was injected, together with helium and neon, into a borehole in the low-diffusivity Opalinus Clay rock. The hydrogen partial pressure was at most 60 mbar. A water production flow rate from the surrounding rock of *c.* 15 ml/day had been obtained previously, indicating that the test interval wall was presumably saturated with water. Helium and neon concentrations decreased as expected while taking into account dissolution and diffusion processes in the porewater. In contrast, the disappearance rate of hydrogen observed (2×10^{-4} to 3×10^{-4} mol/day/m^2) was *c.* 20 times larger than the calculated rate considering only dissolution and diffusion. The same rate was observed following a new hydrogen injection and over a six-month semi-continuous injection phase. Simultaneously, sulphate and iron concentrations decreased in the water, whereas sulphide became detectable. These evolutions may be due to biotic processes involving hydrogen oxidation, sulphate reduction and Fe(III) reduction.

Several national nuclear waste management programmes are considering using steel components in the design of their deep geological repositories for high-level and long-lived radioactive waste. After closure of the underground disposal facility, oxygen will be consumed and anoxic corrosion of steel is expected to produce hydrogen gas. Studies of hydrogen interactions and transfer in argillaceous rocks aim to evaluate what will happen to this hydrogen and how the hydrogen pressure will evolve with time in the underground repositories. Among these studies is the 'Hydrogen Transfer' (HT) experiment, which was installed in 2009 in the Mont Terri Rock Laboratory to determine *in situ* the effective diffusion coefficient of hydrogen in Opalinus Clay. A second objective of this experiment was to evaluate whether a hydrogen reaction with the argillaceous rock can be detected *in situ* at low temperature (15–16 °C) and whether microorganisms play a role in this potential consumption.

The experimental concept of the HT experiment is based on gas circulation within a borehole (Vinsot *et al.* 2008*a*, *b*). After an initial phase during which the rock natural gas and porewater production and composition at the test location were followed up, the first hydrogen injection was performed in June 2011.

This paper describes the design of this *in situ* test and presents the experimental results regarding the evolution of hydrogen concentration in the circulating gas. It also reports the observed seepage

From: Norris, S., Bruno, J., Cathelineau, M., Delage, P., Fairhurst, C., Gaucher, E. C., Höhn, E. H., Kalinichev, A., Lalieux, P. & Sellin, P. (eds) *Clays in Natural and Engineered Barriers for Radioactive Waste Confinement*. Geological Society, London, Special Publications, **400**, http://dx.doi.org/10.1144/SP400.12

water composition evolution. Based on these experimental results, the processes involved in the observed evolution of hydrogen concentration are discussed.

Geological context and rock characteristics

The Mont Terri Rock Laboratory is located in a tunnel in the Jura Mountains, in northwestern Switzerland at a depth of *c.* 300 m below ground level. It is a 'methodological laboratory' (cf. Delay *et al.* 2014) in the Opalinus Clay, which is a Jurassic-age well-consolidated claystone with a hydraulic conductivity below 3×10^{-12} m s^{-1} (Thury & Bossart 1999).

Based on the study of five core samples, the total dry weight percentage of clay minerals (illite, kaolinite, chlorite and illite–smectite mixed layers) varies between 56 and 61 wt%, quartz varies between 12 and 19 wt%, and calcite varies between 10 and 18 wt% at the test location (Fernandez *et al.* 2009; Lerouge *et al.* 2010). Other compounds include feldspars (2–8 wt%), dolomite (2–3 wt%), siderite (0.2–1 wt%), pyrite (0.5–1.4 wt%), organic matter (*c.* 1 wt% organic C) and TiO_2 (0.5 wt%). These values correspond to the ranges described by Pearson *et al.* (2003) over the Opalinus Clay at Mont Terri.

From thin section observations, the rock displays a fine grain fabric with heterogeneities. The clay matrix is formed of particles of less than 1 μm with detrital components (biotite, muscovite and chlorite) of 10–50 μm. It contains automorphic crystals of calcite, dolomite and siderite as well as framboidal pyrites. The heterogeneities are due to the occurrence of fossil debris ranging in size from 50 μm to a few millimetres. The fossil debris includes particles of organic matter, carbonate test and shell fragments, and phosphate elements. Despite a careful search, celestite was not found in the core samples. The $\delta^{13}C$ and $\delta^{18}O$ values measured on calcites vary from −0.8 to −2.0‰ PDB (Pee Dee Belemnite) and from +23.8 to +25.3‰ SMOW (standard mean ocean water), respectively (Lerouge *et al.* 2010).

On the studied core samples, the water content lies between 7.0% and 7.7% by mass (with respect to the dry rock) and the total porosity lies between 17.2% and 18.6% by volume (Lerouge *et al.* 2010). Based on leaching and squeezing tests, the chloride accessible porosity was evaluated to be *c.* 57% of the total porosity (Fernandez *et al.* 2009).

Measurements of exchangeable cations (Na^+, K^+, Mg^{2+}, Ca^{2+}, Sr^{2+}) were made on four core samples (Lerouge *et al.* 2010). The sum of exchangeable cations obtained lies between 14.1 and 15.6 meq/100 g, with site occupancies of *c.* 43.5% for Na^+, 6.5% for K^+, 20% for Mg^{2+} and 30% for Ca^{2+}. The exchangeable Sr^{2+} value was 0.002 meq/100 g.

Experimental methods

Experimental principles

The experimental setup consists of a 15-m-long and 76-mm-diameter inclined ascending borehole, of which the last 5 m constitute the test interval. The borehole is perpendicular to the bedding. The theoretical rock surface area in the test interval is 1.2 m^2. Precautions were taken during the coring and equipment fitting phases to minimize the introduction of microorganisms and to avoid the introduction of organic matter into the borehole. The last 6 m of the borehole were cored with argon as a drilling fluid in order to protect the rock from any contact with atmospheric oxygen (oxidation) and in order to measure the concentration of dissolved nitrogen gas naturally present in the clay rock. Two gas flow lines link the test interval to a gas circulation module, which is located in the drift and allows monitoring of the gas composition. In addition, the gas circulation module makes it possible to inject pure hydrogen at a controlled flow rate.

The gas pressure in the test interval has been set and maintained from the beginning at a value between 1.3 and 2.5 bar. This pressure is much lower than the pore pressure in the surrounding rock. Under the effect of the hydraulic pressure difference between the borehole and the surrounding rock, and in spite of the low hydraulic conductivity of the rock, water flows into the borehole interval, where it accumulates and is then pumped out through a water-sampling line. In the drift, a water-sampling module connected to this line makes it possible to extract the water in order to maintain a constant water column height in the test interval and to monitor the water composition.

Experimental setup

The experimental setup for this test consisted of equipment installed in the ascending borehole BHT-1, a gas circulation module and a water-sampling module (Lettry & Fierz 2009) (Fig. 1). These are described in the following.

Borehole equipment. The borehole equipment consists of a multi-packer completion including a 5-m-long test interval for gas circulation and porewater collection at the far end of the borehole and a 50-cm-long observation interval for measuring pore pressure below the test interval. The observation interval is separated from the test

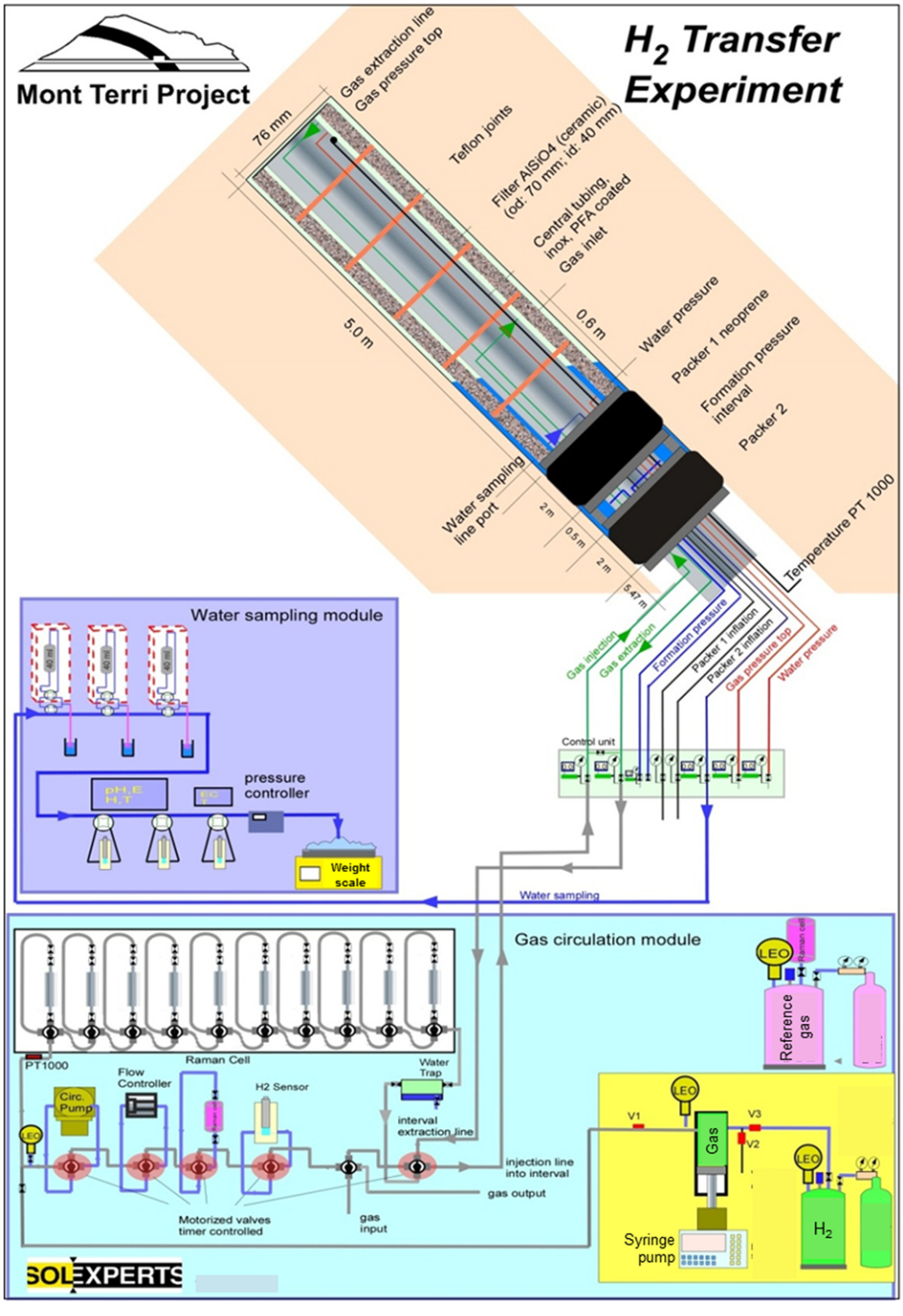

Fig. 1. Experimental layout of the borehole gas injection equipment, the gas circulation system and the water-sampling device.

interval by a 2-m-long packer filled with water (Fig. 1).

The test interval comprises a perfluoroalkoxy (PFA)-coated, stainless steel inner tube (outer diameter OD = 40 mm) fitted with several, 15-mm thick, 42% porosity, $AlSiO_4$ ceramic filter ring sections (OD = 70 mm, inner diameter ID = 40.5 mm). Teflon spacers are fitted between the filter rings. These spacers form barriers in the annular space between the inner tube and the ceramic filters, forcing the gas to circulate in contact with the rock and not just within the annular space. The inner tube and ceramic filter occupy *c.* 60% of the test interval volume, leaving a space of *c.* 9 l for fluids.

The completion has two hydraulic packers. The rubber of the first packer in contact with the test interval is neoprene-covered natural rubber, and that of the second packer is natural rubber alone. Neoprene is used to ensure better chemical inertia than natural rubber and so as not to influence the composition of the water.

Five lines are connected to the test interval: the water-sampling line made of poly-ether-ether-ketone (PEEK) (ID = 1.57 mm) set 12 cm from the packer, the two gas circulation lines made of stainless steel (ID = 2.4 mm) set 72 and 416 cm from the packer, respectively, and three pressure control lines. In the drift, each line is connected to a Keller LEO 3 pressure gauge in a control unit.

Gas circulation module. The gas circulation module includes a KNF circulation pump, a Bronkhorst gas-flow controller (range 0–100 ml min^{-1}), 10 Swagelok stainless-steel sampling cylinders (75 or 150 ml) that can be disconnected to perform gas sample analyses, a HY-OPTIMA 740 by H2scan H_2-specific solid detector probe, and a Teledyne ISCO D-500 gas injection pump. The gas volume in the gas circulation module is *c.* 0.9 l when the ten 75-ml-volume cylinders are online. The gas circulation lines are made of stainless steel with Swagelok fittings. In the gas module, a probe connected to a Raman spectrometer is used to make in-line measurements of the partial pressure of the gases (H_2, N_2 and CH_4) present in sufficient quantities (Lundy & Vinsot 2010). The analyser is a Kaiser Optical Systems Raman Rxn3 spectrometer. The probe used is the Kaiser Optical Systems AirHead model. For H_2, the Raman probe was calibrated with three mixtures of gases comprising 1 vol%, 3 vol% or 5 vol% hydrogen in argon at 1.5 bar and the hydrogen sensor was calibrated with a single mixture of gas comprising 5 vol% hydrogen by varying its pressure between 1.05 and 1.80 bar.

Water-sampling module. The water-sampling module includes an El-Press Bronkhorst water-pressure control device, which regulates the water flow rate, three water-sampling cylinders and a Sartorius weight scale. The water from the borehole passes through the sampling vials before collecting in a 600 ml Tedlar bag standing on the scale. The water-sampling cylinders are made of polytetrafluoroethylene (PTFE)-coated stainless steel or of PEEK. The water lines and the fittings are made of PEEK.

Data acquisition system. All the sensors (pressure, gas flow rate, hydrogen, scale, etc.) are connected to a central database, which acquires and stores the measured values every 5–20 min (Tabani *et al.* 2010).

Chemical analyses

In the laboratory, the water sample cylinders were connected to a special cell to measure the pH without contact with the ambient air. A few millilitres of the water were immediately used for alkalinity measurement by titration. Another 2 ml were immediately transferred into one arm of a two-armed glass vessel, the second arm containing H_3PO_4 (85%). The vessel was then flushed with pure nitrogen and closed. Inclining the vessel caused the H_3PO_4 to mix with the sample, and as a result the CO_2 from all dissolved inorganic carbon compounds was released into the gas phase. The gas phase was then transferred to the evacuated sample loop of the isotope ratio mass spectrometer with dual inlet system for measurement (IRMS, MAT-250; resolution (5% valley), 200; abundance sensitivity, 1.3×10^{-6} for 44/45; high-voltage stability, 1×10^{-5}). The measured results were corrected to carbon standards NBS18–Calcite, NBS19–Calcite, NBS23–$SrCO_3$, IMEP8–CO_2, CO_2–lab standard and Hydroisotop lab standard (DIC). The one sigma error for clean standard material is $\pm 0.2‰$. Results were related to Vienna Pee Dee Belemnite (VPDB) in the delta notation.

Cations Li^+, Na^+, K^+, Mg^{2+}, Ca^{2+} and Sr^{2+} were analysed by a Dionex ion chromatograph using an IonPac CG 12 A, 4 × 50 mm guard column and a CS 12 A, 4 × 250 mm analytical column. Anions Cl^-, NO_3^-, SO_4^{2-}, Br^-, I^-, PO_4^{3-}, $S_2O_3^{2-}$ and acetate were analysed by a Dionex ion chromatograph ICS 1500 using an IonPac AG 22, 4 × 50 mm guard column and an AS 22, 4 × 250 mm analytical column.

NH_4^+ and total sulphide (H_2S, S^{2-}, HS^-) were analysed photometrically. Cr, Fe, Mn, Co, Ni, Cu, Zn, As, Se, Rb, Zr, Nb, Mo, Cs and Ba were analysed by inductively coupled plasma mass spectrometry (ICP-MS).

Gas samples were collected in 25 ml stainless-steel cells. The gas composition was analysed using a Shimadzu GC17A gas chromatograph (GC) equipped with two capillary columns (column 1,

plot fused silica, Molsieve 5A, 50 × 0.53 mm, film thickness df = 50 μm, Varian; column 2, plot fused silica, CP Poraplot Q-HT, 25 × 0.53 mm, df = 10 μm, Varian) and two detectors (detector 1, micro-volume thermal conductivity detector (micro-TCD), VICI Instruments; detector 2, flame ionization detector (FID), Shimadzu). Sample attachment was carried out with a special quick connection (Swagelok), allowing direct connection of the sample cells to the evacuated inlet system of the gas chromatograph (eight-port dual external sample injector, Valco Europe) without contact with the outside atmospheric gases.

The carbon-13 content of the alkanes was analysed by gas chromatography isotope ratio mass spectrometry (GC-IRMS) (MAT-250, Varian MAT; resolution (5% valley) 200; abundance sensitivity, 1.3×10^{-6} for 44/45; high-voltage stability, 1×10^{-5}). The alkanes were oxidized completely to CO_2 in a combustion interface and then measured in the isotope ratio mass spectrometer. Measured results were corrected to carbon standards NBS18–Calcite, IAEA CO–1, NBS23–$SrCO_3$, CO_2–lab standard 1 and CO_2–lab standard 2.

Chronology of the test

Initial phase. The borehole equipment was installed just after drilling. The test interval was then filled with pure argon at a pressure of 2.3 bar and the circulation of this gas was started. The composition of this circulating gas was monitored over almost two years. It was observed that its composition evolved: concentrations of nitrogen, methane and other light alkane up to C6 (hexane) increased with time; helium and CO_2 were also detected. The flow of nitrogen in the test interval was *c.* 0.15 mmol/day over the first year (half of the test). During the same period, the flow of methane was close to 0.019 mmol/day and the flow of ethane was *c.* 0.0016 mmol/day. All of these gases were originally dissolved in the rock porewater. Indeed, their occurrence in Opalinus Clay porewater has been described (Pearson *et al.* 2003; Vinsot *et al.* 2008*a*; Cailteau *et al.* 2011). The surface area of the rock supplying these gases in the test interval was *c.* 1.2 m^2. The ratios between nitrogen, ethane and propane, respectively, and methane deduced from the measured volume fractions were 7.745 for N_2/CH_4, 0.085 for C_2H_6/CH_4 and 0.058 for C_3H_8/CH_4 (Vinsot 2012).

During the year preceding the first injection of hydrogen, the water flow rate from the surrounding rock was between 10 and 20 ml/day into the borehole and the water composition was determined. As the rock surrounding the test interval was homogeneous and not fractured, this flow rate indicated that the wall of the test interval was saturated with water.

Hydrogen injection phase. The first hydrogen injection was performed by replacing the previous circulating gas with a mixture of gases containing 5 vol% H_2, 5 vol% He, 5 vol% Ne and 85 vol% Ar at a total pressure close to 1.5 bar. Because the initial gas was not completely eliminated after the gas replacement operation, the largest hydrogen partial pressure value was close to 0.06 bar. Helium and neon served as reference non-reactive gases because changes in their content should only depend on dissolution and diffusion processes in the rock porewater. As a consequence, they can help to calibrate the transport part in a reactive transport model.

Following this first injection in the test interval, the hydrogen concentration dropped below the detection limit in 65 days. In November 2011, pure hydrogen was added to the circulating gas to obtain, once more, a hydrogen partial pressure of 0.06 bar in the test interval. After this second injection, the added hydrogen disappeared once again in 65 days.

In February 2012, a semi-continuous hydrogen injection phase was launched. This consisted of injecting pure hydrogen regularly to maintain a partial pressure close to 0.06 bar in the test interval.

Hydrogen tightness test. Before the first hydrogen injection, on-site tightness tests were conducted with the gas module alone (i.e. without connection to the borehole) with a mixture of gases comprising 2.2 vol% hydrogen in argon at a total pressure of 1.1 bar over 200 days. The outcome of these tightness tests was an average total gas leak rate of 0.5 mbar/day, corresponding to 0.5 ml/day at standard ambient temperature and pressure (SATP). Hydrogen contributed to 9% of the gas loss. This rate was four times higher than the hydrogen content of the gas, showing that hydrogen leaked more easily than argon. The pure hydrogen leak rate was therefore estimated to be 0.04 mbar/day or 1.6×10^{-6} mol/day.

Experimental results

Gas composition

Between June 2011 and September 2012, 17 gas sampling cylinders were disconnected from the gas module for laboratory analyses (Table 1). New gas sampling cylinders were added three times over this time period – 28 June 2011, 26 August 2011 and 9 February 2012. The added gas sampling cylinders contained pure argon at a pressure between 10 and 20 mbar.

Table 1. *Gas analyses*

Lab no.	–	–	227432	226613	226614	227311	227312	227313	227431	229318	229319
Sampling date	–	–	Gas mixture	10 June 2011	13 June 2011	16 June 2011	21 June 2011	28 June 2011	5 July 2011	15 July 2011	29 July 2011
Sampling time	–	(days)	1	4	7	12	19	26	36	50	76
Total pressure	–	(bar)	1.52	1.52	1.51	1.51	1.51	1.46	1.46	1.45	1.44
Hydrogen	H_2	(vol%)	5.05	3.95	3.85	3.55	3.35	3.18	2.65	2.08	0.52
Helium	He	(vol%)	4.77	4.05	4.01	4	3.9	3.9	3.75	3.65	3.8
Neon	Ne	(vol%)	4.98	3.95	4	4.03	4	3.9	3.75	3.9	3.85
Argon	Ar	(vol%)	85.2	85.7	86.8	87	87.4	87.7	88.5	89	90.1
Oxygen	O_2	(vol%)	< 0.05	< 0.05	< 0.05	< 0.05	< 0.05	< 0.05	< 0.05	< 0.05	< 0.05
Nitrogen	N_2	(vol%)	< 0.05	2.05	1.24	1.2	1.11	1.09	1.09	1.51	1.87
Carbon dioxide	CO_2	(vol%)	< 0.03	0.15	0.03	0.05	0.03	0.03	0.03	0.01	< 0.01
Methane	CH_4	(vpm)	< 1	790	733	895	994	1120	1220	1300	1680
Ethane	C_2H_6	(vpm)	< 1	126	120	149	163	183	209	220	262
Propane	C_3H_8	(vpm)	< 1	126	122	148	161	181	216	216	250
Carbon-13-CH_4	δ^{13}C-CH_4	VPDB‰	–	− 36.9	− 22.7	− 22.7	− 26	− 37.7	− 38.6	− 38.1	− 38.4
Deuterium-H_2	δ^2H-H_2	VSMOW‰	− 850 ± 15	− 864	− 854	− 862	n.a.	n.a.	− 854	n.a.	n.a.

Table 1. (*Continued*)

Lab no.	–	–	231003	231715	233563	233936	233937	234665	236349	240299
Sampling date	–	–	3 November 2011	23 November 2011	9 February 2012	22 February 2012	28 February 2012	24 March 2012	14 May 2012	5 September 2012
Sampling time	–	(days)	147	167	245	258	264	289	340	454
Total pressure	–	(bar)	1.40	1.44	1.40	1.34	1.36	1.36	1.35	1.35
Hydrogen	H_2	(vol%)	< 0.05	2.9	< 0.1	< 0.05	4.9	3.83	2.96	2.86
Helium	He	(vol%)	3.1	2.97	3.05	3.1	2.87	3.1	3.05	2.92
Neon	Ne	(vol%)	3.79	3.7	3.65	3.65	3.5	3.55	3.5	3.35
Argon	Ar	(vol%)	88.8	86	87	86.6	82.3	82.6	82.5	77.4
Oxygen	O_2	(vol%)	< 0.05	< 0.05	< 0.1	< 0.1	< 0.1	< 0.1	< 0.1	< 0.02
Nitrogen	N_2	(vol%)	3.68	3.9	5.5	5.8	5.6	6.1	7.12	12.2
Carbon dioxide	CO_2	(vol%)	0.08	0.012	0.04	0.02	0.02	0.02	0.02	0.09
Methane	CH_4	(vpm)	3200	3600	6000	6700	6400	6700	7900	10300
Ethane	C_2H_6	(vpm)	436	445	550	570	560	595	685	850
Propane	C_3H_8	(vpm)	393	415	452	470	460	475	540	585
Carbon-13-CH_4	δ^{13}C-CH_4	VPDB‰	− 33.1	− 38.5	− 40.3	− 39.8	− 38.4	− 38.7	− 38.8	− 47.9
Deuterium-H_2	δ^2H-H_2	VSMOW‰	n.a.	n.a.	n.a.	n.a.	− 846	− 826	− 835	− 807

The initial time for the calculation of the sampling time corresponded to the date of the first hydrogen injection; vpm, volumic part per million; n.a., not available.

The three methods used for hydrogen monitoring (H_2-specific sensor, Raman spectrometry and gas chromatography analyses performed on gas samples) gave similar results, except when rapid fluctuations affected the gas chromatography and Raman analyses more than the H_2-specific sensor (Fig. 2). Regarding the first hydrogen injection, the concentration of hydrogen, helium and neon at the time of injection was 4.0 ± 0.2vol%; this value was lower than the concentration in the injected gas mixture because the injected gas mixture did not entirely replace the existing gas in the borehole (Vinsot 2012).

Following this injection, the hydrogen vanished completely in 65 days, whereas helium and neon losses were less than 12% of the initial content over the same time period and less than 28% over 454 days (Fig. 3). When pure hydrogen was added to the circulating gas in November 2011, the 0.017 moles of added hydrogen disappeared at the same rate. For both injections, the change in the volume concentration of hydrogen was virtually linear with

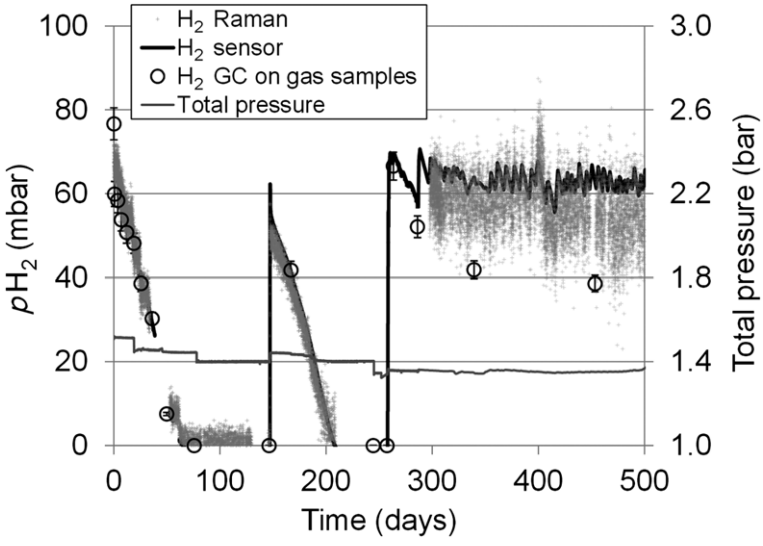

Fig. 2. Hydrogen partial pressure and total pressure measured in the gas.

a slope close to 0.06 vol% per day, corresponding to an average hydrogen loss of *c.* 2.7×10^{-4} mol/day.

Over the semi-continuous hydrogen injection phase started 22 February 2012, the hydrogen partial pressure varied from 40 to 80 mbar. From the beginning of this phase (day 258) until day 454 (date of the last water sampling, 5 September 2012), the quantity of hydrogen added was 0.085 moles (Fig. 4) and the average hydrogen loss rate was 3.3×10^{-4} mol/day.

The hydrogen loss rates observed are two orders of magnitude higher than that of the hydrogen leak rate estimated from the on-site tightness tests. Another tightness test was performed in June 2012. It consisted in bypassing the borehole for a period of 28 h: the hydrogen content value obtained with the specific sensor remained constant over this time period. This result confirmed that the hydrogen loss observed was not due to a leak from the gas module circuit.

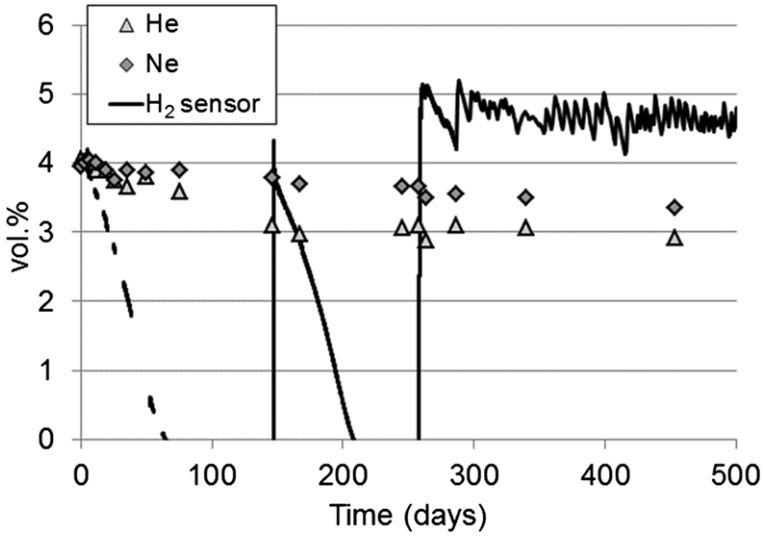

Fig. 3. Volume fraction of helium, neon and hydrogen measured in the gas.

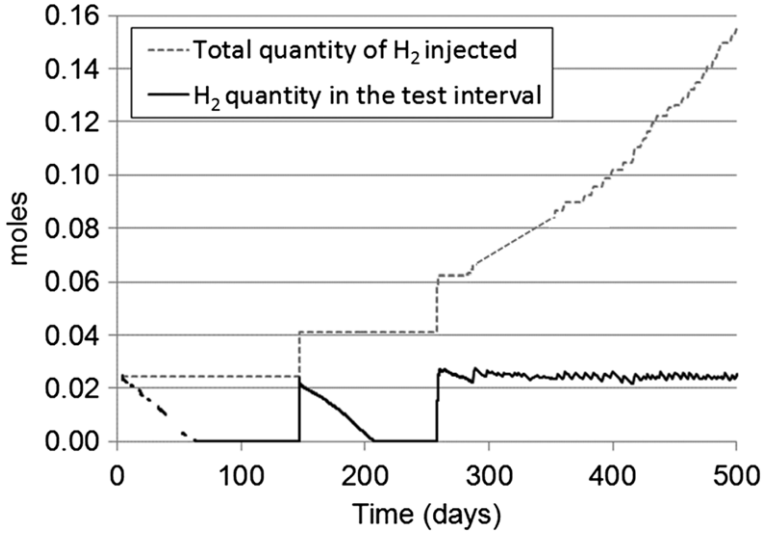

Fig. 4. Evolution of the quantity of hydrogen existing in the test interval and added since the beginning of the test.

Nitrogen and alkane concentrations evolved similarly before and after the first hydrogen injection (Table 1 and Vinsot 2012). N_2/CH_4 and C_2H_6/CH_4 ratios calculated during the hydrogen phase (i.e. after the first hydrogen injection) were equal or slightly bigger than those obtained during the initial phase (i.e. before the first hydrogen injection). During the initial phase, the $\delta^{13}C$ values of methane varied by 3–10‰VPDB when the gas circuit was open for gas extraction or gas injection (Vinsot 2012). Other than during these events, the $\delta^{13}C$ values of methane remained in the range −40.3 to −36.3‰VPDB over the whole test and did not significantly differ between the initial phase and the hydrogen phase.

The CO_2 concentrations measured in the gas were between 0.003 and 0.14 vol%, corresponding to CO_2 partial pressures ranging between 0.08 and 3.4 mbar (log pCO_2 of −4.1 to −2.5). The CO_2 partial pressure was much lower than that calculated from equilibrium with the seepage water using pH, alkalinity and total inorganic carbon (log pCO_2 around −2, cf. Table 2). The measurements of the gases have been checked and are not at issue. The highest values were associated with the events of gas extraction or injection. The processes involved are not yet understood. The measured $\delta^{13}C$ values of CO_2, between −10.1 and −7.5‰VPDB, and the $\delta^{18}O$ values of CO_2, between 30.1 and 34.7‰VSMOW, fit the ranges already described for the Opalinus Clay at Mont Terri (Pearson *et al.* 2003; Girard *et al.* 2005).

The H_2S concentrations measured in the gas were always below the detection limit value (1 vol%).

Water composition

Table 2 presents the results of analyses of eight samples of BHT-1 borehole water. The first sample was taken about 14 months after the start of the experiment by disconnecting an inline vial into which the borehole water had been flowing for almost two months. The second sample was taken after about 26 months, just before the first hydrogen injection. The third sample was taken a little less than one month after the first hydrogen injection. The fourth water sample and the next four water samples were taken before and during the semi-continuous hydrogen injection phase, respectively.

Overall, the samples have similar concentrations of the major species (Fig. 5 and Table 2). The pH measured in the laboratory immediately after opening of the vials is between 6.9 and 7.3 (Fig. 6). The BHT-1 water fits the chloride profile of a NW–SE cross-section of the Mont Terri laboratory derived from a summary of geochemical data in Pearson *et al.* (2003). Based on the Br^-/Cl^- and SO_4^{2-}/Cl^- ratio values, the BHT-1 borehole water corresponds to dilute seawater, like all the water sampled from the Opalinus Clay at Mont Terri (Pearson *et al.* 2003, 2011).

After the first hydrogen injection, the concentrations of sulphate and strontium have decreased a little, together with total iron (Fig. 7). Sulphide was detected only in the last two samples (Table 2).

The strontium isotope ratios of the BHT-1 borehole water were between 0.707651 ± 0.000013 and 0.707770 ± 0.000012 and fall within the range for Mont Terri water, which extends from 0.707651 to

Table 2. *Water analyses and parameters calculated from water composition*

Lab no.	Unit	215145	226615	227433	233659	233935	235660	236066	241154
Sampling date	–	15 June 2010	8 June 2011	5 July 2011	9 February 2012	28 February 2012	21 March 2012	26 April 2012	5 September 2012
Sampling time	(days)	−359	−1	26	245	264	286	322	454
Electrical conductivity (25 °C) Lab	(μS cm^{-1})	30 000	29 800	29 800	29 600	29 600	29 700	29 800	29 400
pH value (20 °C) Lab	–	7.1	7.4	7.2	7.0	7.0	7.0	7.0	6.9
Alkalinity pH4.3	(meq l^{-1})	2.33	2.09	2.15	2.06	1.78	2.00	2.53	2.08
Alkalinity pH3.3	(meq l^{-1})	2.95	2.75	2.8	2.75	2.55	3.33	2.75	2.85
TIC (measured)	(mmol l^{-1})	2.42	2.38	2.45	2.1	1.9	2.7	3.1	2.5
Na	(mol l^{-1})	2.42E-01	2.62E-01	2.67E-01	2.63E-01	2.66E-01	2.53E-01	2.53E-01	2.55E-01
K	(mol l^{-1})	2.14E-03	1.54E-03	1.52E-03	1.60E-03	1.59E-03	1.38E-03	1.39E-03	1.47E-03
Ca	(mol l^{-1})	1.63E-02	1.65E-02	1.65E-02	1.77E-02	1.77E-02	1.62E-02	1.62E-02	1.63E-02
Mg	(mol l^{-1})	1.97E-02	1.87E-02	1.89E-02	1.95E-02	1.93E-02	1.83E-02	1.85E-02	1.86E-02
NH_4	(mol l^{-1})	6.04E-04	6.22E-04	5.83E-04	5.75E-04	5.91E-04	6.16E-04	4.80E-04	5.24E-04
Cl	(mol l^{-1})	2.80E-01	2.93E-01	3.05E-01	3.05E-01	3.08E-01	2.90E-01	2.90E-01	2.95E-01
SO_4	(mol l^{-1})	1.56E-02	1.70E-02	1.70E-02	1.54E-02	1.55E-02	1.51E-02	1.51E-02	1.44E-02
Br	(mol l^{-1})	4.64E-04	4.39E-04	4.34E-04	4.49E-04	4.74E-04	4.27E-04	4.55E-04	4.48E-04
I	(mol l^{-1})	2.17E-05	1.13E-05	1.37E-05	8.84E-06	8.84E-06	6.42E-06	8.03E-06	6.42E-06
S (−II)	(mol l^{-1})	<1.5E-05	<3.0E-06	<1.5E-05	<6.0E-06	<1.5E-05	<1.5E-05	1.11E-04	1.05E-04
Ba	(mol l^{-1})	4.90E-07	3.71E-07	4.09E-07	3.34E-07	3.34E-07	5.94E-07	5.19E-07	4.45E-07
Fe	(mol l^{-1})	1.97E-05	7.85E-05	1.55E-04	2.28E-06	3.84E-06	1.64E-06	2.74E-06	2.92E-06
Li	(mol l^{-1})	6.75E-05	6.76E-05	6.76E-05	6.76E-05	6.91E-05	5.87E-05	6.17E-05	6.17E-05
Mn	(mol l^{-1})	3.34E-06	2.88E-06	4.09E-06	3.71E-06	2.14E-06	3.43E-06	3.34E-06	2.50E-06
Sr	(mol l^{-1})	4.66E-04	5.56E-04	5.58E-04	4.87E-04	4.98E-04	4.01E-04	3.93E-04	3.69E-04
B	(mol l^{-1})	2.26E-04	2.97E-04	3.02E-04	2.12E-04	2.22E-04	3.35E-04	3.44E-04	2.88E-04
Se	(mol l^{-1})	1.70E-06	<7.0E-08	<7.0E-07	2.78E-06	2.45E-06	<7.0E-08	4.39E-07	9.68E-08
Si	(mol l^{-1})	1.94E-04	5.99E-04	7.26E-04	4.90E-04	5.63E-04	5.99E-04	6.89E-04	6.71E-04
DOC	(mol C l^{-1})	6.50E-04	2.42E-03	2.39E-03	2.13E-04	1.28E-03	1.31E-03	1.46E-03	1.07E-03

(*Continued*)

Table 2. *Continued*

Lab no.	Unit	215145	226615	227433	233659	233935	235660	236066	241154
$\delta^{18}O-H_2O$	(‰ VSMOW)	−8.3	−8.53	−8.4	−8.71	−8.68	−8.61	−8.66	−8.46
$\delta^{2}H-H_2O$	(‰ VSMOW)	−51	−53.9	−53	−54	−53.4	−53.4	−53.6	−53.2
$\delta^{13}C-TIC$	(‰ VPDB)	−6.99	−13	−17.6	−15.1	−12.2	−12.6	−14	−17.7
Ionic strength	(M)	3.31E-01	3.46E-01	3.54E-01	3.54E-01	3.56E-01	3.38E-01	3.38E-01	3.41E-01
Charge balance	(%)	0.66	0.8	−0.12	0.26	0.24	0.04	0.16	0.11
Calcite SI	–	−0.06	0.1	0	−0.17	−0.2	−0.11	−0.20	−0.28
Celestite SI	–	−0.05	0.04	0.04	−0.06	−0.05	−0.14	−0.15	−0.19
log pCO_2 (meas. alk)	log(bar)	−2.10	−2.34	−2.23	−2.03	−2.07	−1.95	−2.04	−1.92
log pCO_2 (meas. TIC)	log(bar)	−2.23	−2.42	−2.32	−2.21	−2.25	−2.09	−2.03	−2.04
Dolomite SI	–	−0.01	0.27	0.08	−0.26	−0.34	−0.14	−0.32	−0.48
Strontianite SI	–	−0.78	−0.55	−0.65	−0.9	−0.93	−0.89	−0.99	−1.1
Gypsum SI	–	−0.49	−0.47	−0.47	−0.49	−0.48	−0.51	−0.51	−0.53
Barite SI	–	0.46	0.35	0.39	0.27	0.27	0.52	0.47	0.38
Rhodochrosite SI	–	−1.35	−1.38	−1.27	−1.39	−1.64	−1.33	−1.4	−1.59
Siderite SI	–	−0.73	0.00	0.21	−1.80	−1.61	−1.86	−1.82	−1.86
Br/Cl	(mol/mol)	5.57E-02	5.79E-02	5.57E-02	5.05E-02	5.04E-02	5.19E-02	5.19E-02	4.90E-02
SO_4/Cl	(mol/mol)	1.66E-03	1.50E-03	1.42E-03	1.47E-03	1.54E-03	1.47E-03	1.57E-03	1.52E-03

Presented ionic strength, charge balance, saturations indices and CO_2 partial pressures have been calculated at 15 °C with PHREEQC (Parkhurst & Appelo 1999) using the Thermochimie-V8 database (Duro *et al.* 2012).

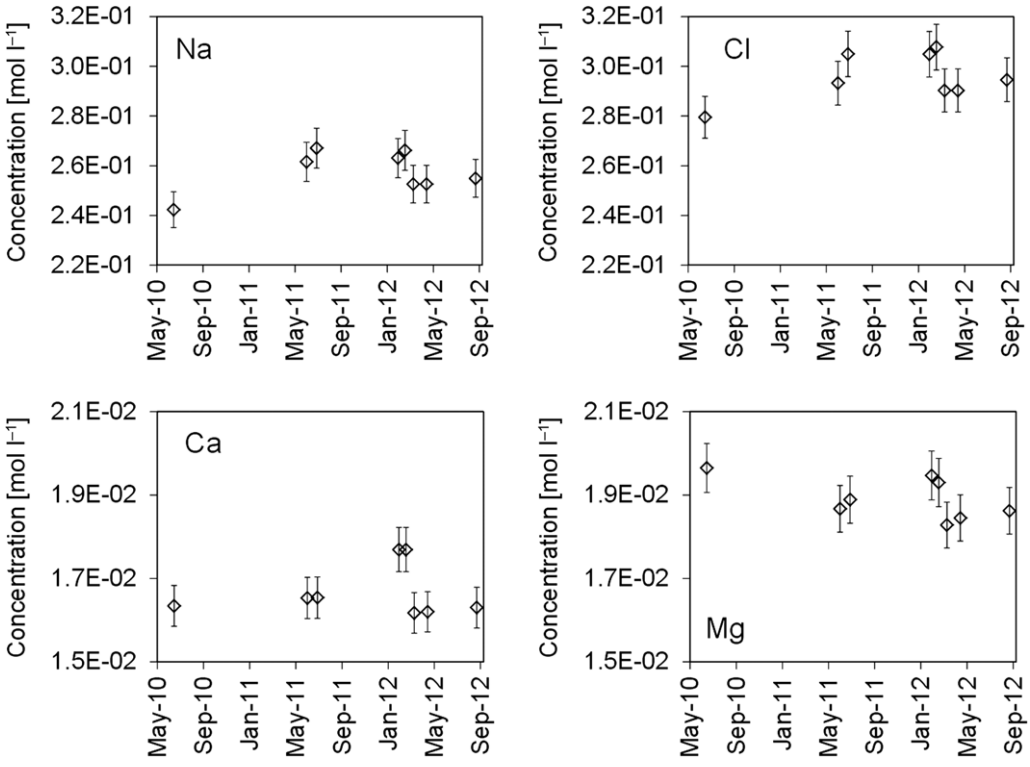

Fig. 5. Evolution of four dissolved species concentrations measured in the borehole water. Error bars represent the uncertainty in the measured values.

0.707774 (Pearson *et al.* 2003). The ratios do not show any specific tendency in their evolution.

The measured $\delta^{13}C$ values of total inorganic carbon (TIC) were between −17 and −7‰ VPDB. The lowest values likely indicate a contribution of oxidized organic matter to the TIC (Girard *et al.* 2005).

Speciation calculations were performed with PHREEQC (Parkhurst & Appelo 1999) and the Thermochimie-V8 database (Duro *et al.* 2012).

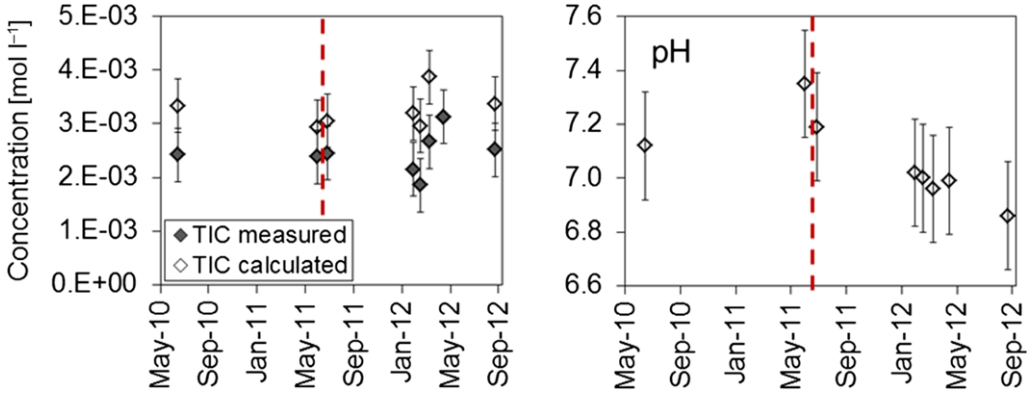

Fig. 6. Evolution of the TIC content and pH in the borehole water. Error bars represent the uncertainty in the values.

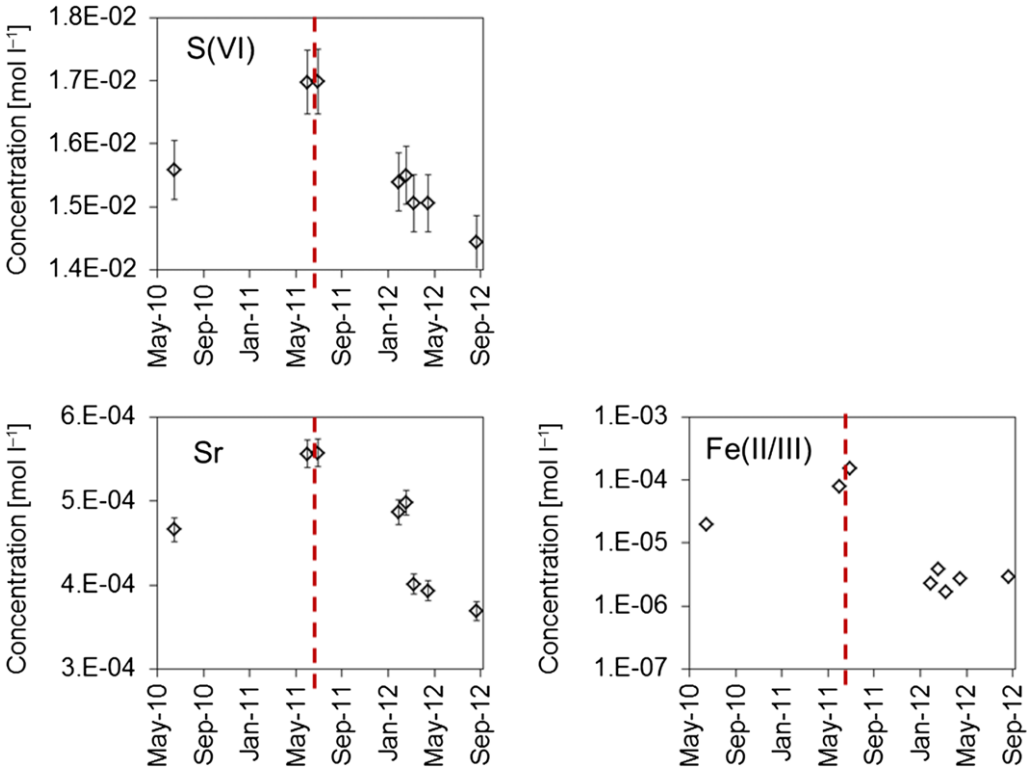

Fig. 7. Evolution of the concentrations of sulphate, strontium and iron measured in the borehole water. Error bars represent the uncertainty in the measured values.

Results are presented in Table 2. The measured alkalinity was used for the calculations. The calculated log pCO_2 values are between −2.4 and −1.7. When available, the measured TIC was used to calculate log pCO_2. The difference between the log pCO_2 values based on measured alkalinity and on measured TIC is smaller than 0.2 (Fig. 8). This shows a rather good internal consistency among the measured pH, TIC and alkalinity values. All the analyses are charge balanced to within 2%. Before hydrogen injection, the sampled water was close to equilibrium with calcite, dolomite and celestite, with almost all the absolute values of the saturation indices with respect to these minerals below 0.1. After the first hydrogen injection, these saturation indices decreased (Fig. 8), but the values obtained remained within the range of uncertainty. Over the experiment, the siderite saturation index varied between −1.9 and 0.2.

The minor species fit with the previous observations summarized by Pearson *et al.* (2003, 2011).

The composition of the BHT-1 seepage water gives complementary insights into the Opalinus Clay porewater, and seems to be in agreement with the current understanding (Pearson *et al.* 2011).

Microbial analyses

Six water samples were taken in sterile glass or plastic tubes between June 2011 and April 2012 to carry out preliminary investigations (using cultural methods) on the microbial population. The results of these investigations show that acetoclastic organisms, sulphate-reducing organisms and thiosulphate-reducing organisms developed over the sampling time period. No methanogens or hydrogenotrophics were found, in spite of a specific search for these organisms.

Discussion

Gases

The evolution of H_2, He and Ne concentrations in the gas was calculated taking into account dissolution and diffusion (Appelo & Vinsot 2012). The modelling was carried out with PHREEQC in a one-dimensional radial configuration, using the multi-component diffusion option (Appelo & Wersin 2007). Diffusion over the water/gas interface at the borehole perimeter was modelled with a

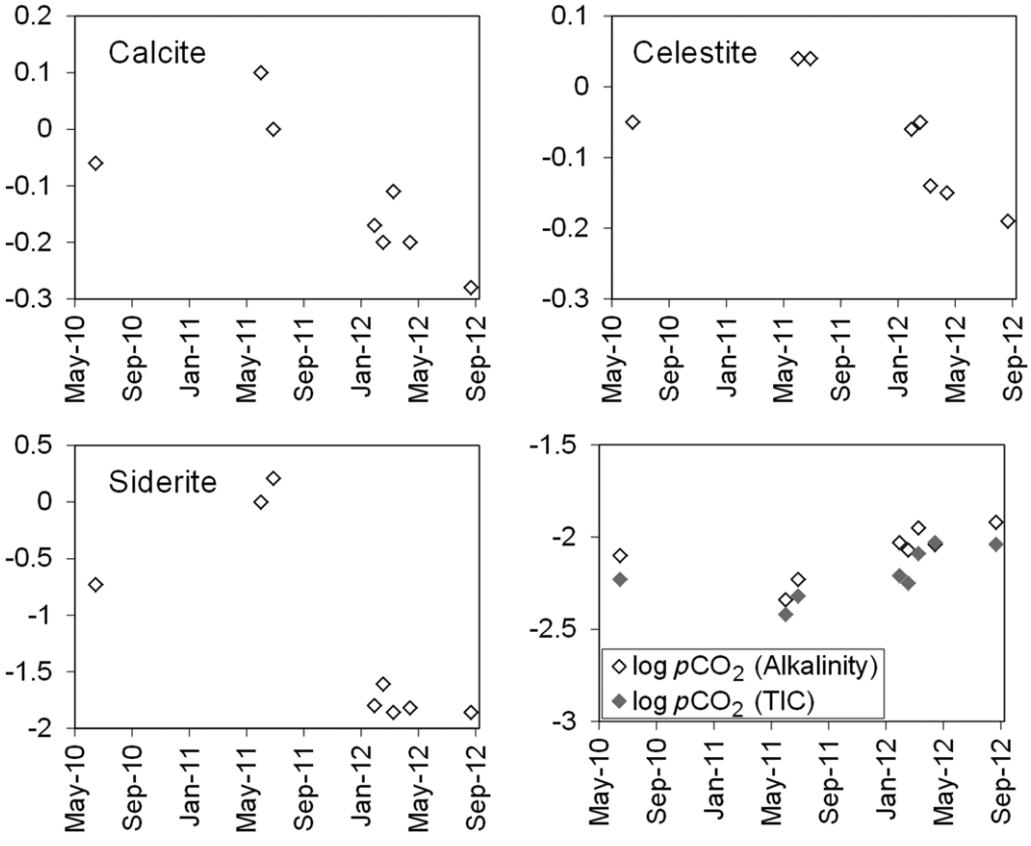

Fig. 8. Saturation indices with respect to calcite, celestite and siderite and log pCO_2 calculated for the borehole water.

two-film model (Liss & Slater 1974). The water-film thickness was assumed to be 0.25 mm (in agreement with calculations for other systems, cf. Appelo & Postma 2005). The Henry constants K_H (atm l mol^{-1}) and diffusion coefficients in water D_w (Jähne *et al.* 1987) are listed in Table 3, together with the effective diffusion coefficients $D_e = \varepsilon D_w/\theta^2$ at 15 °C. Porosity $\varepsilon = 0.16$ and tortuosity factor $\theta^2 = \varepsilon^{-1.1} = 7.5$ were the same for the three dissolved gases. The calculated evolutions were in good agreement with the measured data for neon and slightly above the measured data for helium (Fig. 9). BRGM (2012) tested the influence of the tortuosity value on the calculated evolution of the three gases, but for all the tested values, the decrease in gas concentration rates were still an order of magnitude greater than those observed for hydrogen. In contrast, the measured hydrogen concentration decreased very quickly compared to the model. From these results it appears that the

Table 3. *Solubilities and tracer diffusion coefficients for the gases in the model*

	$-\log K_H$	D_w (10^{-9} m^2 s^{-1})	D_e (10^{-11} m^2 s^{-1})
H_2	3.10	5.13	8.12
He	3.41	7.29	11.53
Ne	3.35	4.04	6.39

The solubilities and diffusion coefficients are for 25 °C; solubilities are corrected to 15 °C using Van't Hoff's equation with a polynomial; diffusion coefficients are corrected by accounting for the viscosity change of water with temperature.

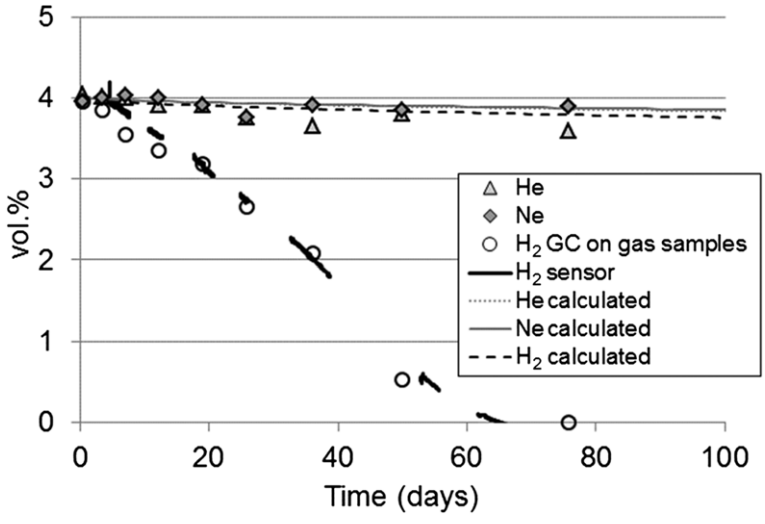

Fig. 9. Observed and calculated evolution of hydrogen, helium and neon over 100 days after the first hydrogen injection.

helium and neon concentration evolutions can be reproduced with a model taking into account dissolution and diffusion in the porewater. The difference observed between the evolution of the helium concentration and the evolution of the neon concentration could be due to a small leak of helium. However, the difference observed between the change in concentration in hydrogen and the change in concentration of helium is evidence of behaviour particular to hydrogen.

The total quantity of hydrogen, summed up to day 454, was *c.* 126 mmoles. The hydrogen quantity consumed due to dissolution and diffusion over the same time period was *c.* 6 mmoles. As a consequence, the loss of *c.* 120 mmoles of hydrogen may be due to another process.

Water

The concentrations of three dissolved species (sulphate, iron and strontium) evolved slightly after hydrogen injection. Furthermore, sulphide was detected in the last two water samples.

The measured concentrations of sulphate, iron and sulphide in the borehole water, together with the water production flow rate, were used to calculate the total quantities that have been lost (sulphate and iron) or gained (sulphide) in the water since the first hydrogen injection. Quantities obtained were *c.* -23 mmoles for sulphate, -1 mmole for iron and $+1$ mmole for sulphide. As a consequence, the average rate of sulphate concentration decrease was *c.* 5×10^{-5} mol/day.

Processes

Biotic and abiotic processes involving hydrogen consumption in argillaceous rocks have been intensively investigated (e.g. Truche *et al.* 2009, 2010; Libert *et al.* 2011; Stucki 2011; Didier *et al.* 2012).

Reaction (1), which consumes hydrogen, sulphate and Fe(II) and produces sulphide, could explain the observed phenomena:

$$4H_2 + SO_4^{2-} + Fe^{2+} = FeS + 4H_2O \qquad (1)$$

Pyrrhotite (FeS) precipitation is thermodynamically possible in the borehole water as the calculated saturation indices (on the two last water samples containing detectable sulphide) were higher than 3.5. Furthermore, this reaction is in a rather good agreement with the observed consumption of *c.* 120 mmoles of hydrogen and 23 mmoles of sulphate, with the mass balance of hydrogen and sulphate having a ratio of 4/1.

The hypothesis that this reaction could describe the observed processes implies that more than 20 mmoles Fe(II) have become available. The iron source is unknown. The ionic exchanger could contribute a part to the Fe(II) needed for the reaction. However, a part of the Fe(II) could also come from Fe(III) reduction.

In any case, these reactions should be controlled by kinetics, as it was shown that the observed data cannot be reproduced with a local equilibrium hypothesis in a reactive transport model (BRGM 2012).

Moreover, these reactions should involve microorganisms, because it was shown that abiotic

reactions did not occur in the experimental conditions (Truche *et al.* 2009, 2010; Didier *et al.* 2012). Hydrogenotrophs have not been identified yet, but this result, based on cultural methods, cannot be considered as a proof of their absence. Iron-reducing bacteria also need to be sought.

This hypothesis corresponds to a preliminary and simplified conclusion. It has to be checked quantitatively, taking into account diffusion. It is also necessary to look for other potential processes.

On the other hand, it can be observed that methane production associated with carbonate reduction by hydrogen did not seem to occur. The N_2/CH_4 and C_2H_6/CH_4 ratios were superior or equal before and after the first H_2 injection, and the $\delta^{13}C$ values of methane remained constant before and after the first H_2 injection.

Conclusion

It has been possible to inject hydrogen into a borehole in the Mont Terri Rock Laboratory, controlling precisely the quantity of hydrogen added. Helium and neon were also injected into the borehole. The evolution of the concentration of these two gases was reproduced with a diffusion model in a one-dimensional radial configuration, considering dissolution and diffusion in the porewater. The effective diffusion coefficient was 11.53×10^{-11} m^2 s^{-1} for helium and 6.39×10^{-11} m^2 s^{-1} for neon. These values are in good agreement with the known transfer properties of the rock.

Hydrogen disappeared much faster than helium. Simultaneously, the evolution of the borehole water composition gave indications that hydrogen could have been consumed by reactions involving sulphate and iron reduction.

These preliminary conclusions need to be confirmed and quantified, with the help of reactive transport modelling. Methods from molecular biology should be used to search for hydrogenotrophic and iron-reducing organisms.

We appreciate fruitful discussions with D. Traber, U. Mäder, E. Valcke, N. Waber, S. Daumas and R. Bernier-Latmani during the Mont Terri geochemical meetings. Many thanks also go to G. Lorenz, T. Fierz, T. Theurillat, P. Tabani, A. Mangeot, P. Delage, A. Garnier, A. Bagnoud and C. Nussbaum for their continuous support of the project. We acknowledge the two anonymous reviewers for their helpful comments.

References

Appelo, C. A. J. & Postma, D. 2005. *Geochemistry, Groundwater and Pollution*. 2nd edn. Balkema, Leiden.

Appelo, C. A. J. & Vinsot, A. 2012. *HT (Hydrogen Transfer) Experiment: Building a Model for Calculating the Diffusion of H_2, He, Ne and Ar in a Borehole in Opalinus Clay*. Mont Terri Project Technical Note **TN2009-40**.

Appelo, C. A. J. & Wersin, P. 2007. Multicomponent diffusion modeling in clay systems with application to the diffusion of tritium, iodide, and sodium in Opalinus clay. *Environmental Science and Technology*, **41**, 5002–5007.

BRGM 2012. *Reactive Modeling Transport of Hydrogen (HT Experiment)*. Mont Terri Project Technical Note **TN2011-31**.

Cailteau, C., Pironon, J., de Donato, Ph., Vinsot, A., Fierz, T., Garnier, C. & Barres, O. 2011. FT-IR metrology aspects for on-line monitoring of CO_2 and CH_4 in underground laboratory conditions. *Analytical Methods*, **3**, 877–887.

Delay, J., Bossart, P. *et al.* 2014. Three decades of Underground Research Laboratories. What have we learned? *In*: Norris, S., Bruno, J. *et al.*. (eds) *Clays in Natural and Engineered Barriers for Radioactive Waste Confinement*. Geological Society, London, Special Publications, **400**. First published online March 5, 2014, http://dx.doi.org/10.1144/SP400.1.

Didier, M., Leone, L., Greneche, J.-M., Giffaut, E. & Charlet, L. 2012. Adsorption of hydrogen gas and redox processes in clays. *Environmental Science and Technology*, **46**, 3574–3579.

Duro, L., Grivé, M. & Giffaut, E. 2012. ThermoChimie, the ANDRA Thermodynamic Database. *MRS Proceedings*, 1475, imrc11-1475-nw35-o71, http://dx.doi.org/10.1557/opl.2012.637.

Fernández, A. M., Melón, A. M. *et al.* 2009. *HT Experiment. Physical, Geochemical and Mineralogical Characterization of the Opalinus Clay at Mont Terri from Core Samples of the Borehole BHT-1 Located in the Gallery 08*. Mont Terri Project Technical Note **TN2009-46**.

Girard, J.-P., Flehoc, C. & Gaucher, E. 2005. Stable isotope composition of CO_2 outgassed from cores of argillites: a simple method to constrain $\delta^{18}O$ of porewater and $\delta^{13}C$ of dissolved carbon in mudrocks. *Applied Geochemistry*, **20**, 713–725.

Jähne, B., Heinz, G. & Dietrich, W. 1987. Measurement of the diffusion coefficients of sparingly soluble gases in water. *Journal of Geophysical Research*, **92**, 10767–10776.

Lerouge, C., Gailhanou-Vigier, H. *et al.* 2010. *HT (Hydrogen Transfer) Experiment: Mineralogy and Geochemistry of Cores of the BHT-1 Borehole*. Mont Terri Project Technical Note **TN2009-45**.

Lettry, Y. & Fierz, T. 2009. *HT (Hydrogen Transfer) Experiment. Description of Surface and Downhole Equipment, Site Instrumentation*. Installation Report. Mont Terri Project Technical Note **TN2009-20**.

Libert, M., Bildstein, O., Esnault, L., Jullien, M. & Sellier, R. 2011. Molecular hydrogen: An abundant energy source for bacterial activity in nuclear waste repositories. *Physics and Chemistry of the Earth A/B/C*, **36**, 1616–1623.

Liss, P. S. & Slater, P. G. 1974. Flux of gases across the air–sea interface. *Nature*, **247**, 181–184.

LUNDY, M. & VINSOT, A. 2010. Implementation of Raman and mass spectrometry for on line measurement of gas composition in boreholes. *In*: ANDRA, (ed.) *Clays in Natural & Engineered Barriers for Radioactive Waste Confinement, 4th International Meeting*, 29 March–1 April 2010, Nantes, France, Abstracts 535–536.

PARKHURST, D. L. & APPELO, C. A. J. 1999. *User's Guide to PHREEQC (version 2) – A Computer Program for Speciation, Batch Reaction, One-Dimensional Transport and Inverse Geochemical Calculations*. *USGS Water Resource Invest* Report **99/4259**.

PEARSON, F. J., TOURNASSAT, C. & GAUCHER, E. C. 2011. Biogeochemical processes in a clay formation *in situ* experiment: Part E – equilibrium controls on chemistry of pore water from the Opalinus Clay, Mont Terri Underground Research Laboratory, Switzerland. *Applied Geochemistry*, **26**, 990–1008.

PEARSON, J., ARCOS, D. *ET AL*. 2003. *Mont Terri Project, Geochemistry of Water in the Opalinus Clay Formation at the Mont Terri Rock Laboratory*. Reports of the Swiss Federal Office for Water and Geology (FOWG), Bern, Geology Series, No. 5.

TABANI, P., HERMAND, G., DELAY, J. & MANGEOT, A. 2010. Geoscientific data acquisition and management system (SAGD) of the Andra Meuse/Haute-Marne research center. *In*: ANDRA, (ed.) *Clays in Natural and Engineered Barriers for Radioactive Waste Confinement, 4th International Meeting*, 29 March–1 April 2010, Nantes, France, Abstracts, 253–254.

THURY, M. & BOSSART, P. 1999. Mont Terri Rock Laboratory. Results of the hydrogeological, geochemical and geotechnical experiments performed in 1996 and 1997. SNHGS Geological Report **23**.

TRUCHE, L., BERGER, G., DESTRIGNEVILLE, C., PAGES, A., GUILLAUME, D., GIFFAUT, E. & JACQUOT, E. 2009. Experimental reduction of aqueous sulphate by hydrogen under hydrothermal conditions: Implication for the nuclear waste storage. *Geochimica Cosmochimica Acta*, **73**, 4824–4835.

TRUCHE, L., BERGER, G., DESTRIGNEVILLE, C., GUILLAUME, D. & GIFFAUT, E. 2010. Kinetics of pyrite to pyrrhotite reduction by hydrogen in calcite buffered solutions between 90 and 180 °C: Implications for nuclear waste disposal. *Geochimica Cosmochimica Acta*, **74**, 2894–2914.

STUCKI, J. W. 2011. A review of the effects of iron redox cycles on smectite properties. *Comptes Rendus Geoscience*, **343**, 199–209.

VINSOT, A. 2012. *Hydrogen Transfer (HT) Experiment, Progress Report*. Mont Terri Project Technical Note **TN 2012-77**.

VINSOT, A., APPELO, C. A. J. *ET AL*. 2008*a*. CO_2 data on gas and pore water sampled *in situ* in the Opalinus Clay at the Mont Terri rock laboratory. *Physics and Chemistry of the Earth*, **33**, S54–S60.

VINSOT, A., METTLER, S. & WECHNER, S. 2008*b*. *In-situ* characterization of the Callovo–Oxfordian pore water composition. *Physics and Chemistry of the Earth*, **33S1**, S75–S86.